Comparison of low-frequency data from co-located receivers using frequency dependent least-squares-subtraction scalars

Kevin W. Hall*
CREWES, University of Calgary
kwhall@ucalgary.ca

and

Gary F. Margrave and Malcolm B. Bertram
University of Calgary, Calgary, Alberta, Canada

Summary

A low-frequency sensor comparison survey was acquired at the University of Calgary's test site near Priddis Alberta in August 2009. Portable calibrated broadband seismometers, analog 3C 10 Hz geophones and two makes of digitial 3C accelerometers were deployed at 1 m receiver line spacing, and used to record weight-drop and EnviroVibe (this report) sources at two source points located 50 m from the end of the receiver lines. This study shows that least-squares-subtraction scalars (LSSS) depend on amplitude, frequency, phase, source-receiver offset, quality of sensor placement in or on the ground. LSSS show good promise for future use in quantitative sensor comparison studies.

Introduction

In August 2009 the University of Calgary had access to eight Nanometrics Trillium 240 seismometers which were destined to be deployed to temporary sites around Alberta as part of a monitoring project. While these units were still in Calgary, it was decided to attempt to compare the low frequency response of 10 Hz geophones to these calibrated seismometers. As an additional experiment, with the co-operation of ION and CGGVeritas, ION Vectorseis and Sercel DSU3 accelerometers were also deployed at the University of Calgary's Priddis test site. The ION spread used Vectorseis units recorded on a Scorpion system, and the Sercel spread used DSU3 sensors recorded on a Sercel 428XL system. The 10 Hz geophone spread was laid out as 80 geophones at 1m spacing to provide more detail of surface motion (Figure 1). Trillium, Vectorseis and DSU3 sensors were set up alongside the geophones at 10 m receiver spacing. Holes were augered for the nail-type geophone/MEMS cases. Shallow holes were dug deep enough to remove top-soil (~20 cm) and cement patio blocks were placed and coarsely leveled in the holes for the seismometers. Seismometers and 3C geophones were oriented inline; accelerometers were aligned to magnetic north.

The sources for this survey were an accelerated weight drop unit fired with and without elastic tensioning bands and the University of Calgary's IVI EnviroVibe at 50 m offsets to the north and south of the receiver lines (Figure 1). With the focus on low frequency, the EnviroVibe was operated well outside its design specifications, and many phase errors were observed in the field for frequencies below ~8 Hz. Sweeps acquired were: 3 Hz and 5 Hz (at 3% and 5% of maximum power) mono-frequency sweeps, and a suite of 2-10 Hz and 2-100 Hz linear sweeps (at 10% of maximum power) with 10, 30 and 50 s sweep lengths. All EnviroVibe data was recorded uncorrelated. Long tapers were used at the low-frequency end of the sweep to prevent damaging the EnviroVibe.

For this initial study, we focused on vertical component data from the uncorrelated 2-10 Hz sweeps. We wish to determine if frequency dependent least-squares-subtraction scalars (LSSS) can provide useful information in regards to sensor comparisons.

Method

The amplitudes of any two data traces (S_1 and S_2), can be matched by multiplying one of the traces by some constant, a. The best-fit constant a can be determined in a least-squares-subtraction sense by defining some number

$$\varepsilon = \sum_k (S_{1k} - aS_{2k})^2 \quad , \tag{1}$$

where k represents individual samples within each data trace. Differentiating ε with respect to a and requiring that the result equal zero gives

$$\frac{1}{2}\frac{\partial \varepsilon}{\partial a} = \sum_k S_{1k}S_{2k} - a\sum_k S_{2k}^2 = 0 \quad . \tag{2}$$

Equation (2) can then be solved for a:

$$a = \frac{\sum_k S_{1k}S_{2k}}{\sum_k S_{2k}^2} \quad , \tag{3}$$

where equation (3) is equivalent to the zero-lag cross-correlation divided by the zero-lag auto-correlation.

In order to investigate amplitude dependence on frequency, data traces were band-pass filtered before calculating the LSSS with a series of 1 Hz wide bandpass filter windows from 2-10 Hz in 0.1 Hz increments.

Data preparation

We were unable to use the raw uncorrelated data as originally intended for three main reasons: 1) while three of the recording systems sampled the wavefield at a 2 ms sample rate, the seismometer data were sampled at 10 ms, 2) seismometer data were continuously recorded (no trigger) and 3) the Sercel/DSU3 system was manually triggered for each shot (no time-break).

Source gathers were extracted from the seismometer data using the time of shot recorded in the Aries observer's notes. Time zero was arbitrarily set to 100 ms. The seismometer gathers were then de-biased and re-sampled to a 2 ms sample rate to match the other datasets. De-biasing was required since low frequency components (less than 1 Hz) in the seismometer data were truncated when the gathers were extracted, resulting in an apparent DC bias.

Accelerometer data were integrated to obtain velocity curves. Geophone and accelerometer data were filtered (2-10 Hz) to attenuate higher frequency source, generator and power-line noise, then aligned to the seismometer traces by calculating maximum positive cross-correlations and sub-sample shifting the traces (Figure 2). The data compare well visually, but minor differences can be seen throughout the sweep and the seismometer response is noticeably different at the end of the sweep (right side; Figure 2).

Results

Figure 3 shows receiver gathers of the LSSS calculated for all 2-10 Hz sweeps at the northern SP (For Figures 3 and 4, the LSSS plotted at 5 Hz is the result from equation (3) for input traces filtered with a 4.5-5.5 Hz pass-band). Subtle differences are present in the LSSS for different length sweeps. Dashed lines in Figure 3 have the same slope, and highlight a source-receiver offset dependence of the LSSS. Data from the southern SP exhibit an opposite slope (not shown). Black rectangles highlight a LSSS anomaly 90 m from the northern SP. This anomaly can be clearly seen on the geophone and Vectorseis versus seismometer comparisons, but is less clear on the DSU3 comparison. Figure 4 shows the averaged LSSS curves for all 2-10 Hz sweeps (both source points).

Conclusions

Our results show that the LSSS is frequency dependent (Figures 3 and 4). The fact that the LSSS anomaly 90 m south of the northern source point is seen to a greater or lesser extent on all three comparison plots (Figure 3) may imply that the quality of the seismometer placement at this location was somehow different than at adjacent stations. The dashed lines in Figure 3 highlight source-receiver offset dependent effects in the LSSS. Variations from a horizontal line for averaged accelerometer versus seismometer comparisons (Figure 4) are interpreted to be due to subtle phase variations in the recorded data based on synthetic data results (not shown).

The averaged geophone versus seismometer LSSS curve looks quite different than the Vectorseis and DSU3 curves, which are similar (Figure 4). This is interpreted to mean that we are seeing differences between accelerometer and geophone response below 10 Hz. Differences in scale may be due to differences in units (eg. V vs. μV), and/or the fact that the trace weighting factor was not applied when reading SEGY data files.
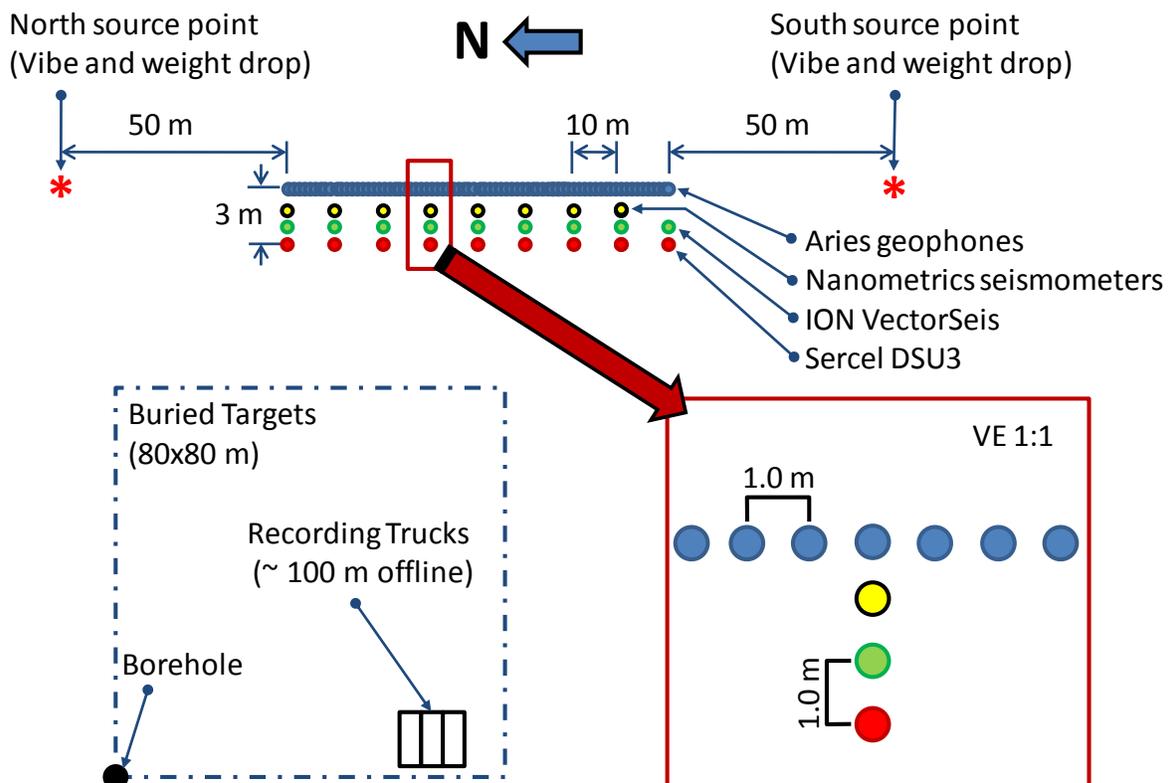
Acknowledgements

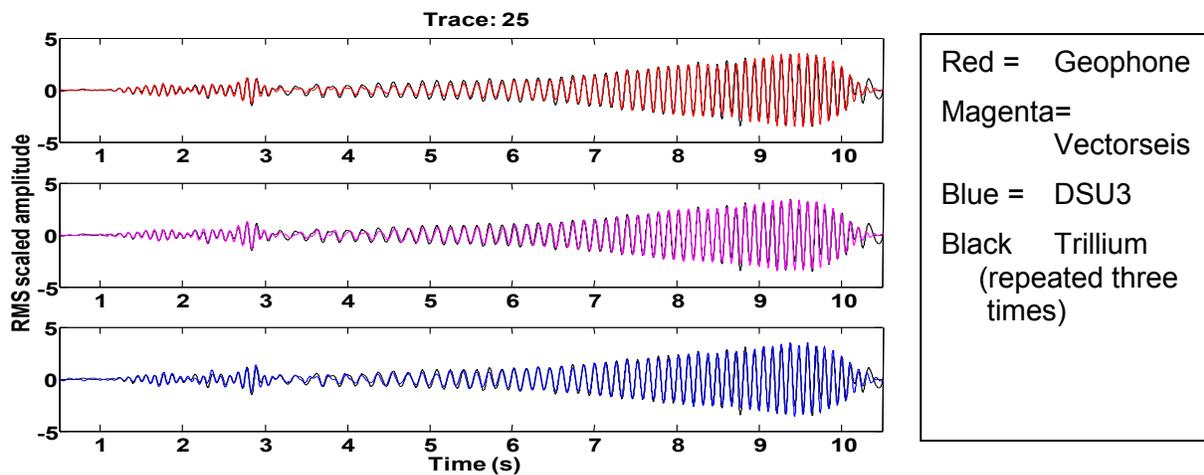Figure 1. Schematic of survey layout at the Univeristy of Calgary's Priddis test site.

Figure 2. Vertical component uncorrelated traces from 50 m south of the north SP for a 10 s 2-10 Hz sweep.
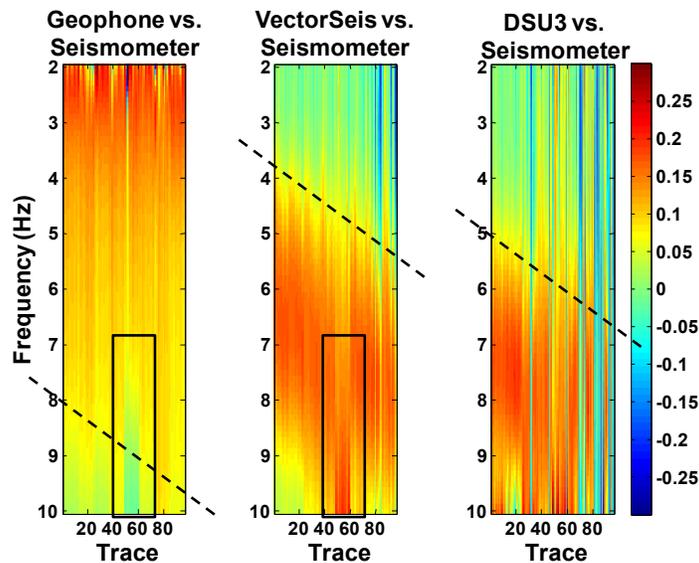

Figure 3. Receiver gathers of least-squares-subtraction scalars (LSSS) for all 2-10 Hz sweeps acquired at the north SP, normalized for display.
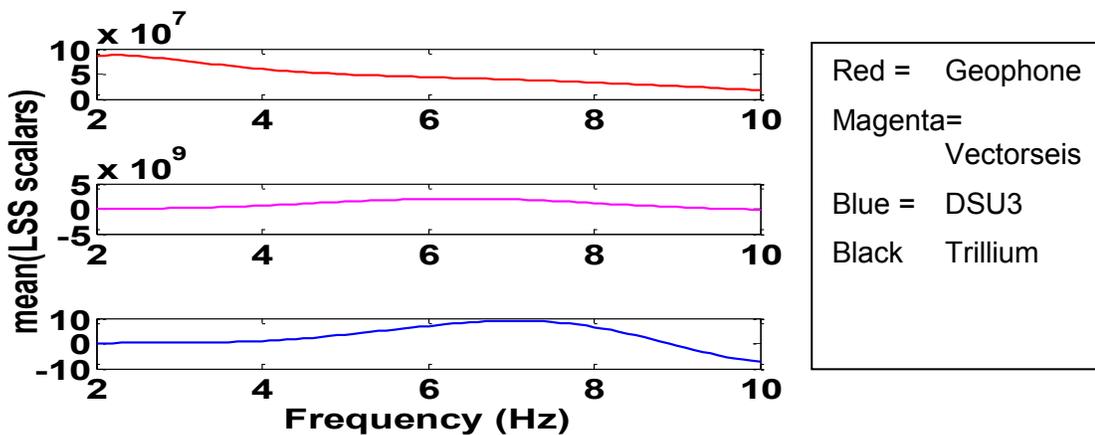

Figure 4. Averaged LSSS for all sensors and for all 2-10 Hz sweeps.